AAS 12-101

EFFECTS OF STAGGERING FORMATION MANEUVERS ON THE MAGNETOSPHERIC MULTI-SCALE MISSION TRAJECTORIES

Khashayar Parsay*, Laurie Mann†

Formation maneuvering for the MMS mission is accomplished by executing a two-burn transfer for each spacecraft to achieve a set of desired states. Because the same radio frequency is shared by all four spacecraft, only one spacecraft can execute a maneuver at any given time. Therefore, the maneuver execution epochs for the MMS spacecraft must be staggered. The selection of the staggered maneuver sequence has a significant effect on the propellant usage and the spacecraft close-approach profile. A method for selecting a favorable maneuver sequence is proposed and measured in terms of propellant and safety.

INTRODUCTION

The primary scientific objective of the MMS mission is to study the phenomenon of magnetic reconnection within the Earth's magnetosphere. To accomplish this objective, the MMS mission configuration comprises four identical spinning spacecraft. These spacecraft form a tetrahedron formation within a predefined region of scientific interest. This region of interest (RoI) is designated as all portions of the orbit above a specified orbit radius. The MMS mission is divided into two main science phases to examine different regions of the magnetosphere. Phase 1 employs a 1.2 $R_E \times 12$ R_E orbit with apogee on the day side of the magnetosphere (the RoI for Phase 1 is above 9 R_E), and Phase 2 employs a 1.2 $R_E \times 25$ R_E orbit with apogee on the night side of the magnetosphere (the RoI for Phase 2 is above 15 R_E). The period of the orbits associated with Phase 1 is approximately 1 day, and the period of those associated with Phase 2 is approximately 2.8 days.[1]

The tetrahedron formation is necessary to resolve both temporal and spatial variations of the magnetic reconnection phenomenon. The goodness of the formation is determined by a quality factor that specifies how closely the four spacecraft resemble, in scale size and shape, a regular tetrahedron when the formation is within the RoI. The scale size, a measure of tetrahedron side length, varies substantially, ranging from 10 km to 400 km. Because the spacecraft orbit in formation, maneuvers are required for the one or more of the following reasons: 1) to re-establish a degraded formation, 2) to avoid a close approach, 3) to change the size of the formation, or 4) to maintain a required perigee height. A formation maneuver for a particular spacecraft is composed of two-burn Lambert transfer, where the first burn is located on the inbound leg of the trajectory and the second burn is located on the outbound leg.

Previous MMS trajectory simulations assumed that all the spacecraft performed their required maneuvers simultaneously. This assumption is denoted as a *non-staggered maneuver sequence*. Because of communication limitations from the spacecraft to ground stations on Earth as well as

*Aerospace Engineer, a.i. solutions, Inc., Lanham, MD 20706.
†Senior Aerospace Engineer, a.i. solutions, Inc., Lanham, MD 20706.

a requirement to remain in contact during a maneuver event, only one spacecraft is allowed to execute a maneuver at a time. Therefore, maneuver operations need to be staggered between spacecraft. Each of the four MMS spacecraft is allocated a time interval in which to perform its inbound burn. These four intervals are consecutive. Each spacecraft is also allocated another time interval to perform its outbound burn; these intervals are also consecutive. The particular order in which the spacecraft are allotted in these intervals is known as the *staggered maneuver sequence*. The staggered maneuver sequence has a significant impact on the propellant expended during the formation maneuver activities as well as the safety of the spacecraft (e.g., the close approach probability) and is the focus of this investigation.

This paper examines the impact of maneuver staggering for Phase 1 of the mission. The staggering problem statement is defined and the solution space for the maneuver sequence selection is described. Criteria for selecting a favorable staggered maneuver sequence based on remaining propellant and close-approach distance are presented. Results based on employing those criteria for selecting a staggered sequence are also examined.

PROBLEM STATEMENT

MMS formation maneuvers cannot be executed simultaneously and need to be staggered in time as only one spacecraft can be in contact with the ground at a given time. A total of 75 minutes is currently allocated for each spacecraft's contact with the Deep-Space Network (DSN) to allow for ground preparation (contact acquisition, command upload and validation, etc.) and for the execution of the orbit and attitude maneuvers. Each spacecraft performs a total of two maneuvers (or burns) to achieve its desired state (position and velocity) determined by the Formation Design Algorithm (FDA).[2,3,4] FDA designs a tetrahedron formation within the RoI about a selected spacecraft known as the *reference* spacecraft. Recall that for Phase 1, the RoI is defined as the region where the reference orbit radius is above 9 R_E.

A typical Phase 1 formation maintenance maneuver for a single MMS spacecraft is illustrated in Figure 1. In this example, the first burn, indicated by $\Delta\mathbf{v}_1$, is located outside the RoI and the second burn, $\Delta\mathbf{v}_2$ is located at apogee. In this two-burn Lambert transfer, the spacecraft is shifted from the current orbit (a dashed curve), to a transfer trajectory (the orange curve) and onto a final orbit (the solid black ellipse). Motion of the vehicle along the orbit is counter-clockwise in the figure.

For most formation maneuvers in Phase 1 and Phase 2, only three of the four spacecraft perform formation maneuvers to achieve the desired orbit states; the reference spacecraft does not perform an orbit maneuver. This strategy lessens the operational burden and reduces the propellant required to maintain the formation. Consequently, there are three burns in each set of formation maneuvers; first set includes the inbound burns for the three maneuvering spacecraft while the second set includes the outbound burns. As a result, each formation maneuver comprises of a total of six burns. In this investigation, the burns are modeled as impulsive because most maintenance maneuvers are small and executed relatively far from perigee. In reality, each spacecraft possesses radial and axial thrusters. Because the spacecraft are spinning at 3 rpm, a "burn" is actually composed of multiple thruster firings to achieve the desired $\Delta\mathbf{v}$ or $\Delta\mathbf{h}$. Note that even though the reference spacecraft does not perform any orbit change maneuver, it will perform an attitude correction maneuver. Therefore, the reference spacecraft is also assigned a staggered maneuver time interval where it can be in contact with the ground station during $\Delta\mathbf{h}$ activity.

A sample MMS maneuver staggering concept for Phase 1 appears in Figure 2. In the figure, each

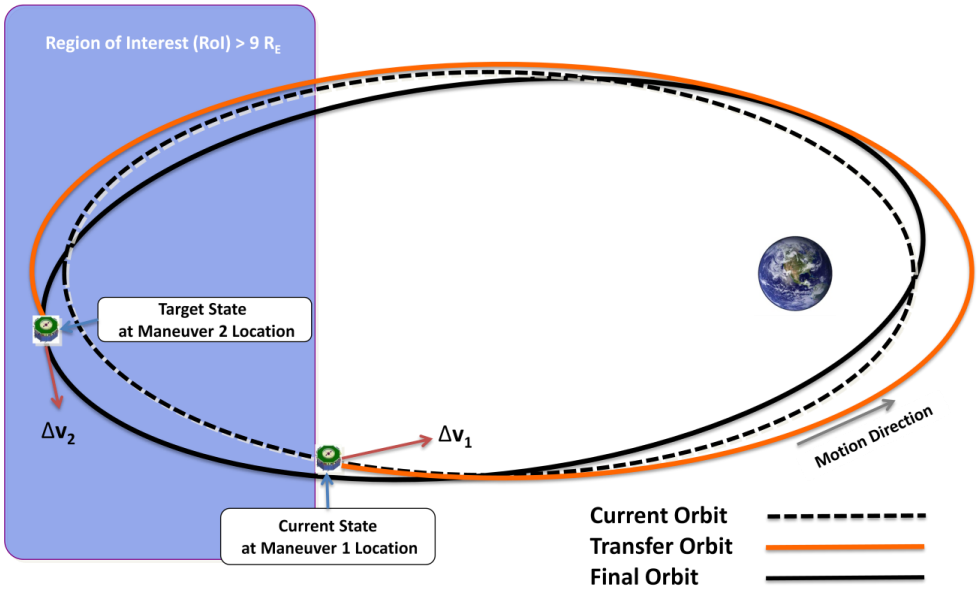

Figure 1. MMS two-burn maneuver

maneuver set consists of four impulsive maneuver epochs that are 75 minutes apart (not shown to scale). The maneuver epochs are denoted by ${}^{q}t_p$, $p = 1, \ldots, 4$ and $q = 1, 2$, where p corresponds to the four available maneuver epochs and q corresponds to the inbound and outbound maneuver sets, respectively. A maneuver sequence defines the *order* in which the spacecraft are maneuvered on the inbound and outbound burns of the formation maneuver. The maneuver sequences within the inbound and outbound burn sets are not necessarily the same. For example, the $\{\text{inbound}\ ,\ \text{outbound}\}$ order could be $m = \{\text{sc}_1, \text{sc}_4, \text{sc}_2, \text{sc}_3\ ,\ \text{sc}_4, \text{sc}_3, \text{sc}_1, \text{sc}_2\}$ corresponding to the impulsive maneuver epochs $\left\{{}^{1}t_1, {}^{1}t_2, {}^{1}t_3, {}^{1}t_4\ ,\ {}^{2}t_1, {}^{2}t_2, {}^{2}t_3, {}^{2}t_4\right\}$.

Because the formation is composed of 4 spacecraft, the total number of permutations of the burn-locations per maneuver set is 24 $(4!)$. Consequently, there is a total of 576 $(4! \times 4!)$ possible staggered maneuver sequences. This set of 576 possible maneuver sequences is denoted M, that is,

$$M := \{m_1, \ldots, m_j, \ldots, m_{576}\} \tag{1}$$

where m_j is the j^{th} possible maneuver sequence for the set M. Each m_j corresponds to a different two point boundary value problem (TPBVP). Therefore, each sequence has a different propellant consumption and associated close-approach profile between the two maneuver sets. Using the previous investigations and results, the non-staggered case is also considered and denoted m_0 as a benchmark for this study. For this non-staggered sequence, all the inbound burns occur at the same time, T_1, and all of the outbound burns occur at T_2.

SELECTING A MANEUVER SEQUENCE

In this investigation, a simulation developed in FreeFlyer® generates and examines all 577 individual TPBVP sets (576 staggered and 1 non-staggered) for a given maneuver.* For each maneuver sequence, the total impulsive Δv and the minimum range between each spacecraft pair bounded by

*FreeFlyer is a mission design Commercial Off The Shelf (COTS) tool.

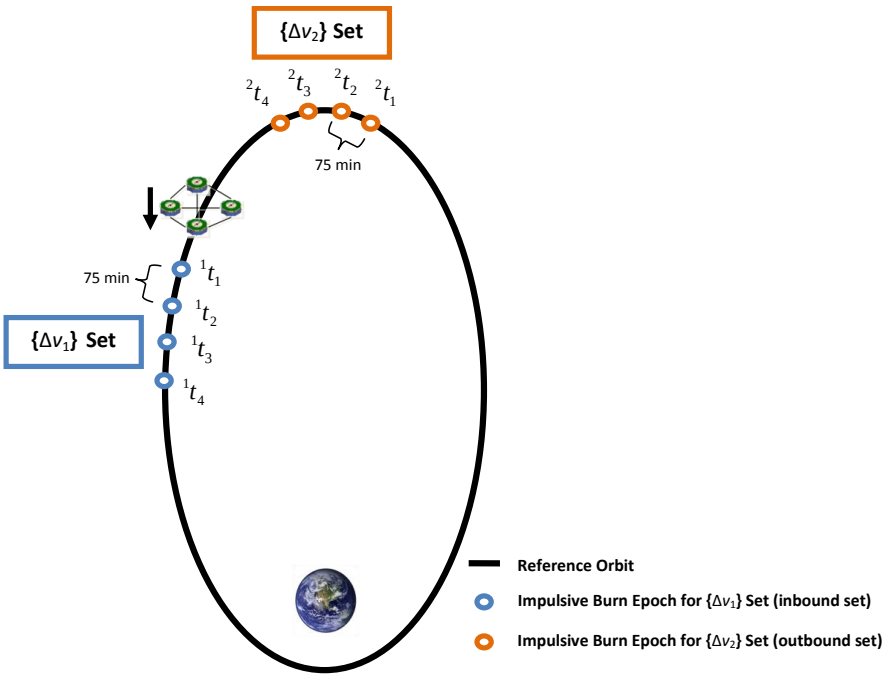

Figure 2. Phase 1 burn locations

the inbound and outbound sets is recorded. This simulation retrieves maneuvers that were planned and executed in the MMS End-to-End trajectories simulations to supply a representative MMS data set.[5] The current MMS End-to-End code simulates the spacecraft trajectories from launch to disposal and includes all required maneuvers in the presence of maneuver execution and orbit knowledge errors. The MMS End-to-End maneuvers are currently modeled as non-staggered maneuvers.

Two assumptions are made in this simulation. First, the vehicle with the lowest amount of propellant is selected as the reference spacecraft to balance remaining propellant across all spacecraft throughout the remainder of the mission. Second, maneuver execution errors, navigation knowledge errors and contingency scenarios are not considered. Since this is a first attempt at understanding the maneuver staggering problem as applied to MMS, non-nominal scenarios will be addressed in future work.

The selection of a favorable maneuver sequence is similar in its challenges to a multi-objective optimization problem. The method presented in this paper employs a series of metric-based filtering processes that define a maneuver sequence subset $F \subseteq M$ from which to refine the solution. The current method selects a favorable sequence through a three step process that defines three nested subsets F_1, F_2, and F_3. The two metrics determined to have the greatest effect on mission lifetime and safety during a formation maneuver activity are the propellant consumption metric and the inter-spacecraft distance metric, respectively.

Propellant Consumption Metric

For every formation maneuver, the total propellant cost for all three maneuvering spacecraft, Δv_T, is selected as the propellant metric and is defined as

$$\Delta v_T = \sum_{\substack{k=1 \\ k \neq n}}^{4} (\Delta v_1 + \Delta v_2)_k \tag{2}$$

where Δv_1 and Δv_2 are the magnitude of the change in velocity vectors for the two-burn method, k is the index of the maneuvering spacecraft, and n is the index of the non-maneuvering spacecraft. Note that each maneuver sequence j can correspond to a different total propellant cost of Δv_{T_j} where $j = 1, \ldots, 576$. Propellant cost and Δv are used interchangeably as they are directly related.

Distance Metric

A total of six inter-spacecraft distances, called side lengths, must be considered for a close-approach evaluation. Let $d_i(t)$ represent the side length for the i^{th} side of the tetrahedron formation at time t, where t falls within the start of the first maneuver set ${}^1t_1$ to the end of the second maneuver set ${}^2t_4$ (see Figure 2). Then, ${}^{\min}d_i$ denotes the minimum side length for the i^{th} side of formation in $t \in \left[{}^1t_1, {}^2t_4\right]$, that is,

$$\begin{aligned} {}^{\min}d_i &= \min d_i(t) \\ t &\in \left[{}^1t_1, {}^2t_4\right] \end{aligned} \tag{3}$$

For each maneuver sequence m_j, the lowest minimum distance that the tetrahedron formation achieves within ${}^1t_1$ to ${}^2t_4$ is denoted by S_j, that is,

$$\begin{aligned} S_j &= \min \left\{ {}^{\min}d_i \right\}_j \\ i &= 1, \ldots, 6 \\ j &= 1, \ldots, 576 \\ t &\in \left[{}^1t_1, {}^2t_4\right] \end{aligned} \tag{4}$$

In summary, each of the maneuver sequences m_j is characterized using the propellant and the safety metrics given by

$$m_j : \left(\Delta v_{T_j}, S_j\right) \tag{5}$$

One of the goals of this study is to understand the effect of maneuver staggering in relation to the non-staggered maneuvers that were calculated in the current version of the End-to-End simulation. Consequently, the non-staggered sequence, $m_0 : (\Delta v_{T_0}, S_0)$, is used as the benchmark maneuver sequence for comparison purposes.

Maneuver Sequence Selection Process

Based on the prioritization of the propellant consumption metric and the distance metric, a process that first discards the maneuver sequences with high Δv_T, then selects the sequences with the safest separation distances, and finally selects the sequence with the lowest Δv_T out of the remaining

sequences is employed. The three-step selection technique is called Propellant-Safety-Propellant (PSP). In the first step, a new subset $F_1 \subseteq M$ is defined as all the maneuver sequences such that

$$\begin{aligned} F_1 :&= \left\{ m_j \mid \Delta v_{T_j} < \Delta v_{T_0},\ m_j \in M \right\} \\ j &= 1, \ldots, 576 \end{aligned} \tag{6}$$

Then, in step 2, a new subset $F_2 \subseteq F_1$ is defined as the set of maneuver sequences within subset F_1 that have the highest S value (S_{max}) and, therefore, are deemed safe.

$$\begin{aligned} F_2 :&= \{ m_r \mid S_r = S_{max},\ m_r \in F_1 \} \\ r &= 1, \ldots, dim\,(F_1) \end{aligned} \tag{7}$$

where r indicates the indices for the maneuver sequences in the subset F_1. The last step is completed by selecting the sequence in F_2 with the lowest Δv_T to populate F_3. If the subset F_1 is empty, 20 maneuver sequences with the lowest Δv_T are chosen. The final maneuver sequence selected generally saves propellant relative to the non-staggered case while assuring safety using the S value distance metric. A flow chart of the process appears in Figure 3.

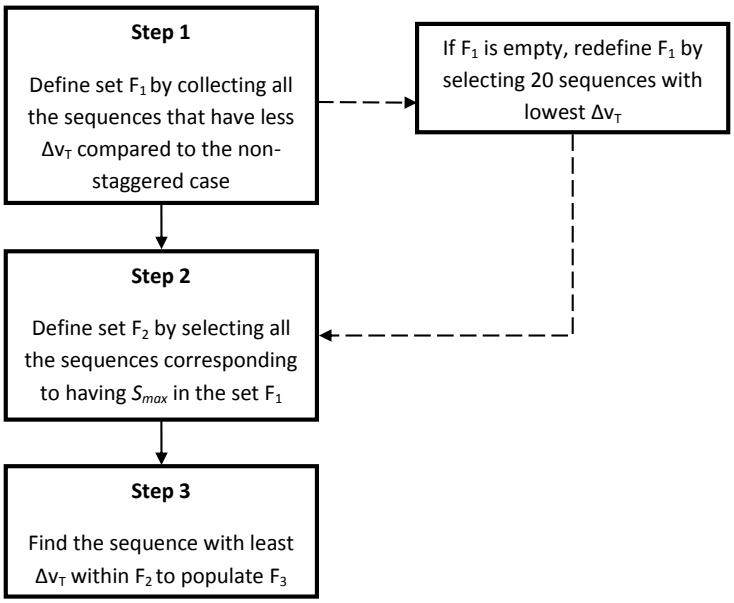

Figure 3. Maneuver Sequence Selection Process By PSP Method

An example of the PSP selection process for an arbitrary maneuver drawn from the End-to-End data appears in Figure 4. The region colored in green and denoted as the *favorable region* is the set of sequences which have both better propellant and safety metrics values than the non-staggered maneuver sequence m_0. The non-staggered case is indicated by a black dot. Figure 4(a) show all the 576 staggered maneuver sequences represented by their respective $\left(\Delta v_{T_j}, S_j\right)$ values. In Step 1, all the cases with $\Delta v_{T_j} > \Delta v_{T_0}$ are discarded, as seen in Figure 4(b). In Step 2, all the sequences with $S < S_{max}$ are discarded, as shown in Figure 4(c). The last step of the PSP method in selecting the final maneuver sequence is shown in Figure 4(d), where the sequence requiring the least amount

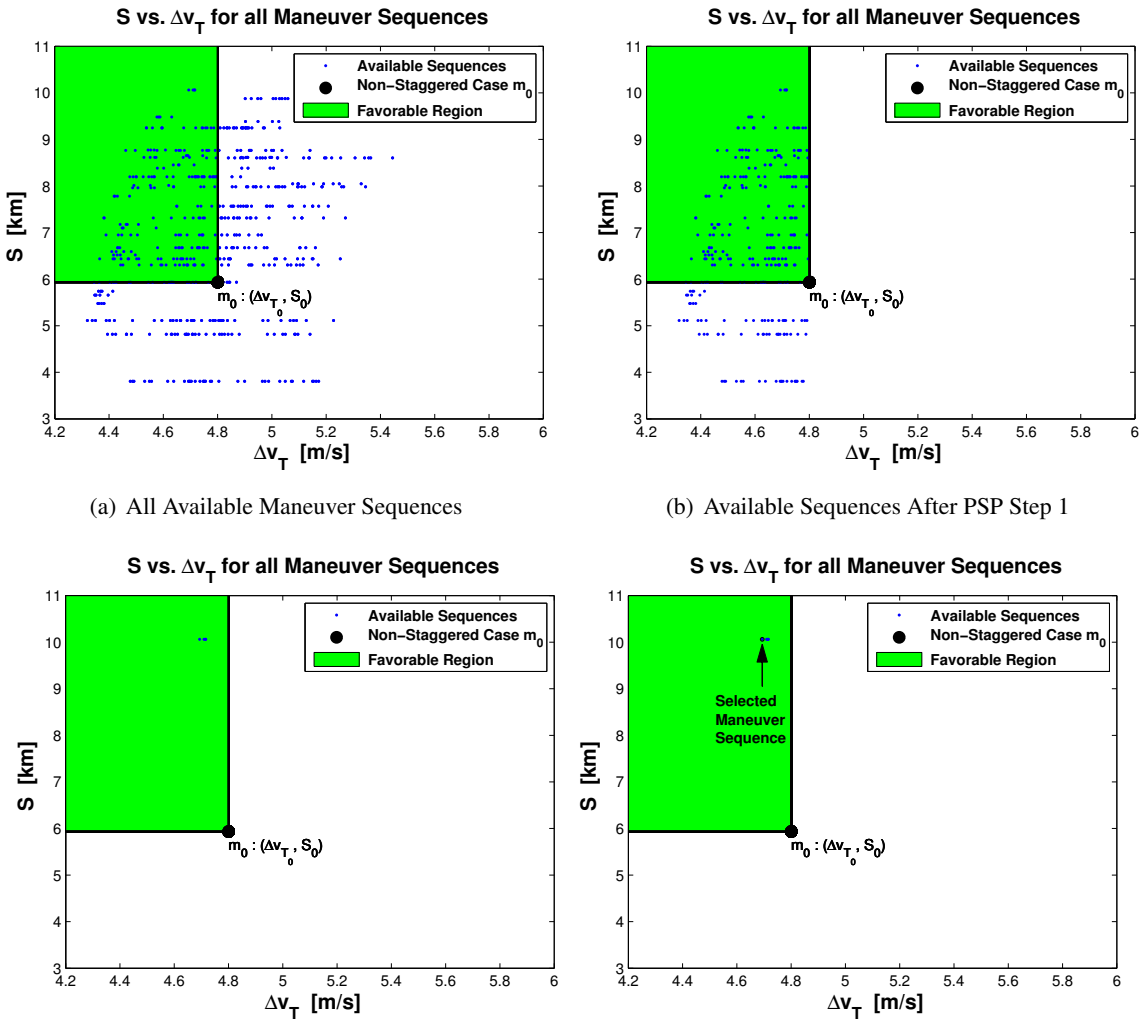

(a) All Available Maneuver Sequences

(b) Available Sequences After PSP Step 1

(c) Available Sequences After PSP Step 2

(d) Selected Maneuver Sequence

Figure 4. PSP Maneuver Sequence Selection Method Example

of Δv_T is selected from a family of solutions with equivalent S values. This final step is explained best using an example. Consider the following two maneuver sequences:

$$m_1 = \{\text{sc}_1, \text{sc}_4, \text{sc}_2, \text{sc}_3 \quad , \quad \text{sc}_4, \text{sc}_3, \text{sc}_1, \text{sc}_2\} \tag{8a}$$

$$m_2 = \{\text{sc}_1, \text{sc}_4, \text{sc}_2, \text{sc}_3 \quad , \quad \text{sc}_4, \text{sc}_3, \text{sc}_2, \text{sc}_1\} \tag{8b}$$

Note that the two sequences are almost identical except that the order of the last two maneuvers differs. If the closest approach occurs before the last two maneuvers, then both sequences have the same S value. However, the sequence m_1 may require less propellant than the sequence m_2. Therefore, the sequence m_1 is selected over m_2.

RESULTS

The effects of maneuver staggering is studied for the 10 km and 25 km formation sizes in Phase 1. These formation sizes are acknowledged as the most challenging in terms of close approach safety.

Out of 80 End-to-End Monte Carlo simulations, total of 224 formation maneuvers for the 10 km formation size and 375 formation maneuvers for the 25 km formation size are selected to assess whether a staggered sequence is an improvement over a non-staggered sequence in terms of propellant and safety. For each formation maneuver selected, a favorable maneuver sequence is identified using the PSP method. For the 10 km formation size, it is demonstrated that for 182 maneuvers out of the 224 maneuvers considered (81.25%), each has at least one maneuver sequence that is more propellant efficient and also has a higher S value relative to the non-staggered maneuver sequence m_0. For the remaining 18.75%, the maneuver sequence selected by the PSP method is either less propellant efficient or has a smaller S value relative to the maneuver sequence m_0. Similar results are observed for the 25 km formation size.

To quantify the highest propellant savings that can be achieved when properly selecting the maneuver staggering sequence, the sequence with the lowest Δv_T is selected for every formation maneuver and the percentage of propellant savings relative to non-staggered Δv_{T_0} is plotted in the histograms appearing in Figure 5. The propellant savings due to maneuver staggering is determined to be on average 9% relative to the non-staggered Δv_{T_0}. In both Figures 5(a) and 5(b), a few PSP solutions, represented by the bars on the far right side of the plots, are less propellant efficient relative to the non-staggered case. These exceptions illustrate that a particular formation maneuver may have no staggered maneuver sequence that is more propellant efficient relative to the non-staggered case.

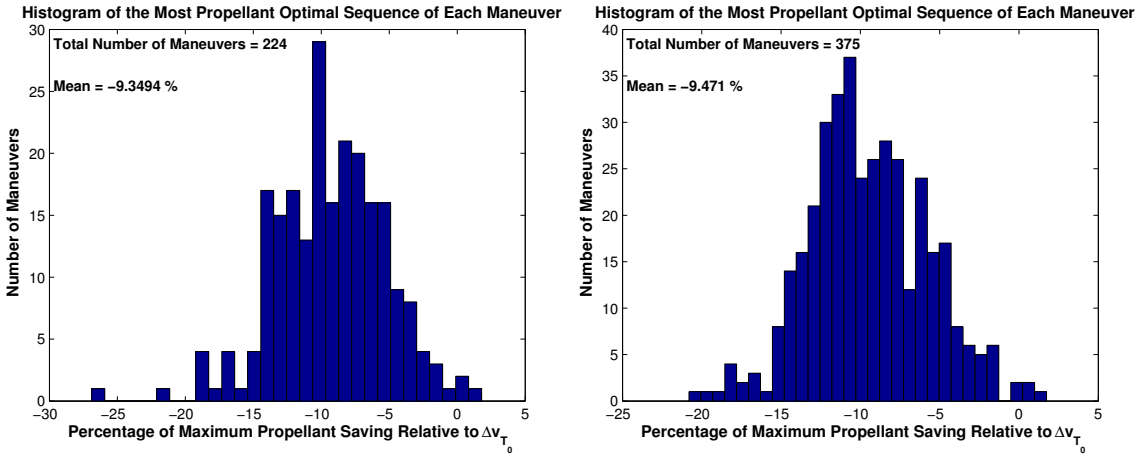

(a) 10 km Formation Size

(b) 25 km Formation Size

Figure 5. Propellant saving for selecting the best propellant optimal maneuver sequence

To understand the negative impact of maneuver staggering in terms of propellant, the maneuver sequence with the largest Δv_T is selected for each maneuver and the percentage difference relative to Δv_{T_0} is plotted in the Figure 6 histograms for both the 10 and 25 km formation sizes. The highest propellant penalty due to maneuver staggering is determined to be on average 26% relative to Δv_{T_0}. This effect demonstrates the importance of selecting a favorable maneuver sequence in terms of propellant and that selecting a random sequence can lead to significant variation in propellant expense.

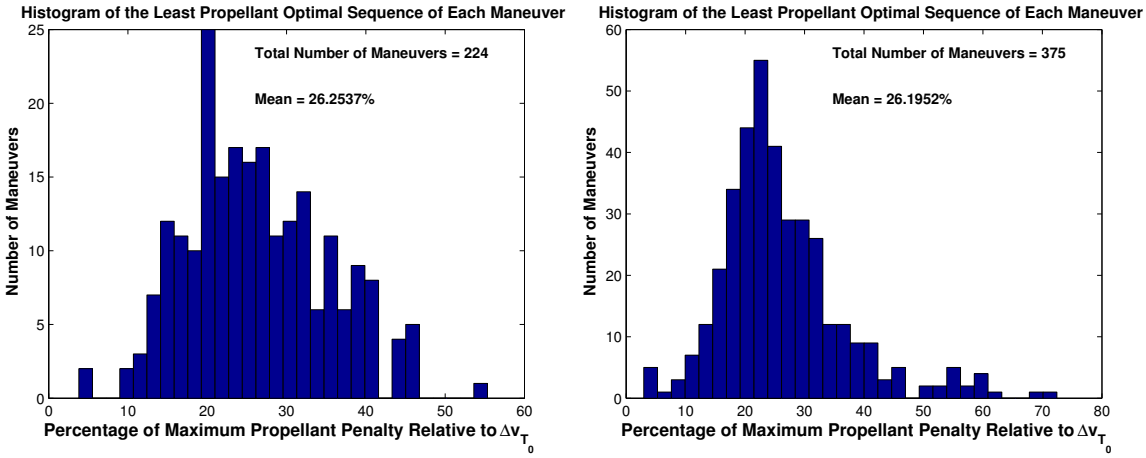

(a) 10 km Formation Size

(b) 25 km Formation Size

Figure 6. Propellant penalty for selecting the least propellant optimal maneuver sequence

CONCLUSION

This study examines the impact of staggering the maneuver epochs for Phase 1 of the MMS mission and provides a preliminary strategy for selecting the a favorable staggering sequence for the MMS mission. It is shown that, for approximately 80% of the formation maneuvers executed in the End-to-End simulation (for the 10 and 25 km formation sizes), there exists at least one maneuver sequence that saves propellant expended *and* increases the minimum inter-spacecraft range, as long as the maneuvers are staggered in time instead of executed simultaneously. Future work will investigate whether the current selection process is valid in presence of maneuver execution and knowledge errors as well as contingency scenarios.

ACKNOWLEDGEMENT

This research was supported by the NASA GSFC under Contract NNG10CP02C, Task Order 23. The authors would like to thank Dr. Conrad Schiff from NASA Goddard Space Flight Center and Dr. Geoffrey Wawrzyniak for their technical inputs and guidance.

NOTATION

Symbols

d_i	i^{th} side of the tetrahedron formation
R_E	Earth radius, km
m	A particular maneuver sequence
M	Set of all possible maneuver sequences available for a formation maneuver
S_j	Lowest minimum side of tetrahedron between the two maneuver sets for the j^{th} maneuver sequence, km
$\Delta\mathbf{v}$	Change in velocity vector, km/s
$\Delta\mathbf{h}$	Change in specific angular momentum vector, km^2/s
Δv	Magnitude of change in velocity vector, km/s
Δv_T	Total Δv budget for three maneuvering spacecraft using Lambert method, km/s

Acronyms

dim	Dimension of a set
FDA	Formation Design Algorithm
PSP	Propellant-Safety-Propellant method for selecting a favorable maneuver sequence
RoI	Region of Interest
TPBVP	Two-Point Boundary-Value Problem
sc$_i$	The i^{th} spacecraft

REFERENCES

[1] C. Gramling, "Overview of the Magnetospheric Multiscale Formation Flying Mission," *AAS/AIAA Astrodynamics Specialist Conference,Pittsburg PA*, 9-13 August 2009.

[2] S. Hughes, "General Method for Optimal Guidance of Spacecraft Formations," *Journal of Guidance, Control, and Dynamics, Vol. 31, No. 2*, March-April 2008.

[3] S. Hughes, "Formation Design and Sensitivity Analysis for the Magnetospheric Multiscale Mission (MMS)," *AIAA/AAS Astrodynamics Specialist Conference, Honolulu, HI*, August 18-21 2008.

[4] L. Mann, K. Parsay, T. Williams, and W. Yu, "Comparison of Magnetospheric MultiScale (MMS) Formation Design Algorithms," *4th International Conference on Formation Flying, Montreal QUEBEC*, May 18-20 2011.

[5] C. Schiff and E. Dove, "Monte Carlo Simulations of the Formation Flying Dynamics for the Magnetospheric Multiscale (MMS) Mission," *22nd ISSFD, Sao Jose Dos Campos, Brazil*, February 28 - March 04, 2011.